Carbohydrate Research 345 (2010) 1802–1807

Contents lists available at ScienceDirect

Carbohydrate Research

journal homepage: www.elsevier.com/locate/carres

Molecular mobility studies on the amorphous state of disaccharides. I—thermally stimulated currents and differential scanning calorimetry

Susana S. Pinto [a], Hermínio P. Diogo [a,*], Teresa G. Nunes [a], Joaquim J. Moura Ramos [b]

[a] Centro de Química Estrutural, Complexo I, IST, TULisbon, Av. Rovisco Pais 1049-001 Lisboa, Portugal
[b] CQFM—Centro de Química-Física Molecular and IN—Institute of Nanoscience and Nanotechnology, Instituto Superior Técnico, TULisbon, 1049-001 Lisboa, Portugal

ARTICLE INFO

Article history:
Received 23 April 2010
Accepted 24 May 2010
Available online 27 May 2010

Keywords:
Molecular mobility
Glass transition
TSDC
Gentiobiose
Cellobiose
β-Relaxation

ABSTRACT

The relaxational processes in amorphous solid gentiobiose and cellobiose are studied by thermally stimulated depolarization currents (TSDC) in the temperature region from 108 K up to 423 K. The slow molecular mobility was characterized in the crystal and in the glassy state. The features of different motional components of the secondary relaxation have been monitored as a function of time as the glass structurally relaxes on aging. It is concluded that some modes of motion of this mobility are aging independent, while others are affected by aging. The value of the steepness index or fragility (T_g–normalized temperature dependence of the relaxation time) was obtained by differential scanning calorimetry (DSC) from the analysis of the scanning rate dependency of T_g.

1. Introduction

The use of carbohydrates in biopreservation,[1,2] particularly in the cryopreservation of cells, has revived research on this important class of biomolecules. Moreover, carbohydrates are recently considered as green raw materials for the chemical industry.[3] Both crystalline and amorphous states are important in the field of food and pharmaceutical technology. The amorphous form of drugs and excipients is of pharmaceutical interest since it has been reported to improve solubility, accelerate dissolution and bioavailability, and promote therapeutic activity.[4,5] There is a general idea that as long as the temperature remains below T_g, some undesirable chemical reactions that lead to deterioration may not proceed. However, evidence does exist that even below T_g there are amorphous materials that still exhibit significant molecular mobility.[6,7] In the glassy state the system is in a non-equilibrium state, with respect to both crystalline and 'equilibrium' glassy state.[6] As a consequence, it will evolve at a rate that depends on the temperature and the thermal history of the glass; the evolution that occurs below the glass transition temperature is referred to as structural relaxation or physical aging.[8] Thus, in order to prevent the molecular processes responsible for destabilization of an amorphous substance over the normal life-time of a pharmaceutical or food product, we need to know the time scales of molecular motion under a variety of conditions.[9] Furthermore, the mobility associated to the secondary relaxations is believed to be related to the protective and chemical stabilization activities during thermal stress.[10]

Gentiobiose and cellobiose are reducing disaccharides consisting of two units of D-glucose linked, respectively, by a β(1→6) and a β(1→4) glycosidic bond (Fig. 1). Cellobiose is produced from cellulose using specific bacterial enzymes and is hydrolyzed by cellobiosidase and cellulose. Humans cannot hydrolyze cellobiose and because of this non-digestibility in human intestines, cellobiose is fermented by intestinal microbes, promoting a good balance of intestinal microflora and decreasing gastrointestinal infections.[11,12] The detection and quantification of cellobiose are important in food and beverage industries and in alternative energy research.[13] Gentiobiose, on the other hand is found to be incorporated into the chemical structure of crocin, the chemical compound that gives saffron color.[14]

Furthermore, cellobiose and gentiobiose are structurally related to trehalose, also a disaccharide with a linkage between two D-glucose units. In this context, we have recently studied by thermally stimulated depolarization currents (TSDC) the slow molecular mobility in amorphous glucose[15] and trehalose.[16] The study of the slow molecular mobility in structurally related molecules, and the characterization of the glass transition in those substances, will help us understand the ability of some sugars for biopreservation. This paper reports our investigation on the temperature dependency of the relaxation time in the amorphous state of cellobiose and gentiobiose by thermally depolarization currents (TSDC), and a complete characterization of the glass transition of these two glass formers by differential scanning calorimetry (DSC). From

* Corresponding author.
E-mail address: hdiogo@ist.utl.pt (H.P. Diogo).

0008-6215/$ - see front matter © 2010 Elsevier Ltd. All rights reserved.
doi:10.1016/j.carres.2010.05.023

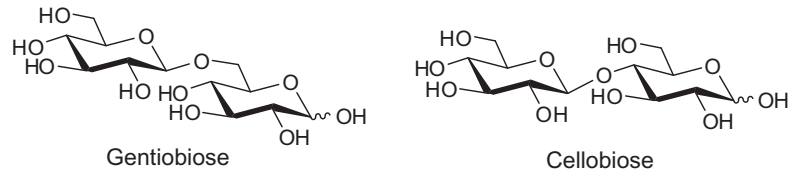

Figure 1. Chemical structures of gentiobiose (left) and cellobiose (right).

these results the time scales for molecular mobility of these disaccharides in the supercooled and glassy states, as well as in the crystalline state, are characterized.

2. Materials and methods

2.1. Materials

D-Gentiobiose or 6-*O*-β-D-glucopyranosyl-D-glucopyranose, CAS number [554-91-6], purity better than 98%, was from Biochemika (lot number 1202873). D-cellobiose or 4-*O*-β-D-glucopyranosyl-D-glucopyranose, CAS number [528-50-7], purity better than 98%, was from Acros Organics. The chemical formula is $C_{12}H_{22}O_{11}$ for both substances, and the molecular weight MW = 342.30 g·mol^{-1}.

The FT-IR spectra from 4000 to 600 cm^{-1} obtained for both crystalline substances are in good agreement with the ones previously reported.[17] Moreover, the absence of the band at 1680 cm^{-1}, which is attributed to water bending, is an indication of the low water content of the samples.

Elemental analysis led to the following results for the mass fractions of C and H in $C_{12}H_{22}O_{11}$ (average of two determinations). Calcd: C, 42.11, H, 6.48. Found for gentiobiose: C, 42.46; H, 7.61. Found for cellobiose: C, 41.90; H, 6.76.

X-ray powder diffraction analysis (XRPD) of the samples was carried out over the range $5° < 2\theta < 35°$, on a D8 Brucker employing a Cu Kα-radiation. Elemental analysis was obtained with a Fisions Instrument EA1108 apparatus. The Fourier-transform infrared spectra (FT-IR) of the samples were recorded in KBr disks, using a Jasco 430 spectrophotometer calibrated with polystyrene film. The XRPD powder pattern obtained for crystalline cellobiose was indexed in space group $P2_1$ with $a = 1096.0(8)$ pm, $b = 1303.6(7)$ pm, $c = 508.7(8)$ pm, $\beta = 90.74°$ in good agreement with those previously obtained by single crystal X-ray diffraction at 25 °C ($a = (1097.2 \pm 0.004)$ pm, $b = (1304.8 \pm 0.005)$ pm, $c = (509.1 \pm 0.003)$ pm, $\beta = (90.83 \pm 0.05)°$).[18]

Amorphous gentiobiose was obtained by quenching from the melt, and amorphous cellobiose was prepared by freeze drying a 0.083 M aqueous solution using a Lyoalfa commercial apparatus, model 6-80, provided by Telstar Industrial, Barcelone, Spain. The cellobiose solution was first frozen in liquid nitrogen, and the primary drying was carried out for 20 h at $-(82 \pm 5)$ °C under a vacuum of 10^{-2} mbar. The sample was subsequently dried in an oven at ≈100 °C for one day to remove residual water. The substances are kept at room temperature inside a desiccator over P_2O_5 for several days before the DSC and TSDC measurements. XRPD data collected for lyophilized cellobiose and quenched gentiobiose did not show any Bragg peaks associated with the lattice geometry, which ensured that the samples were amorphous. A glove box was used to fill the DSC crucibles with the sample and to crimp them.

2.2. Methods

Thermally stimulated depolarization current (TSDC) experiments were carried out with a TSC/RMA spectrometer (TherMold, Stamford, CT, USA) covering the range from −170 to +400 °C. For TSDC measurements the sample was placed between the electrodes of a parallel plane capacitor with an effective area of ~38 mm^2 (thickness of ~0.5 mm). The sample is immersed in an atmosphere of high purity helium (1.1 bar). The fact that the relaxation time of the motional processes is temperature dependent and becomes longer as the temperature decreases enables to immobilize them by cooling. This is the basis of the TSDC technique, which is particularly adequate to probe slow molecular motions. In order to analyze specific regions of the TSDC spectrum, different methods of polarizing the sample can be used, namely the so-called TSDC global polarization experiment and the partial polarization (PP) experiment (often called thermal sampling, windowing, or cleaning). The PP method, where the polarizing field is applied in a narrow temperature interval, enables to resolve a global peak into its individual relaxation modes.[19] The thermal sampling procedure allows to retain (or to freeze) a polarization that arises from a narrow variety of dipolar motions. In the limit of a very narrow polarization window, the retained polarization (and, of course, the current peak that is the result of a partial polarization (PP) experiment) would correspond to a single, individual dipolar motion.[19,20] Several references explaining the physical background of TSDC are available.[21–24] Moreover, several papers are helpful explaining the experimental procedures used in TSDC and the physical meaning of the data provided by this technique.[19,20,25,26] Particularly, supporting materials attached to Ref. 16 can be useful to readers not familiar with the TSDC technique.

The differential scanning calorimetry (DSC) measurements were performed with a 2920 MDSC system from TA Instruments Inc. The samples of ~8–15 mg were introduced in aluminum pans, hermetically sealed using a sample encapsulating press. The measuring cell was continually purged with high purity helium gas at 30 mL/min. An empty aluminum pan, identical to that used for the sample, was used as reference. The baseline was calibrated scanning the temperature domain of the experiments with an empty pan. The temperature calibration was performed taking the onset of the endothermic melting peak of several calibration standards. The temperature calibration for the different heating rates was performed considering the heating rate dependence of the onset temperature of the melting peak of indium and benzoic acid, as explained elsewhere.[27] The enthalpy scale was also calibrated using indium (enthalpy of fusion: $\Delta_{fus}H = 28.71$ J g^{-1}).

3. Results and discussion

The DSC melting peak of our samples of gentiobiose occurred with an onset at $T_{on} = (185.2 \pm 0.1)$ °C and a maximum intensity at $T_{max} = (194.9 \pm 0.2)$ °C, which compares well with the value of the melting temperature $T_m = 196$ °C reported in the literature.[28] In this work the melting enthalpy was $\Delta_{fus}H = (54.7 \pm 0.5)$ kJ mol^{-1} (average of six values). The calorimetric glass transition temperature was found to be $T_g = 86$ °C (on heating at 10 °C min^{-1}), significantly lower compared with the value $T_g = 100.8$ °C found in the literature.[28] The heat capacity jump at the glass transition is $\Delta C_p = (0.73 \pm 0.01)$ J K^{-1} g^{-1} = (249.9 ± 3.4) kJ mol^{-1} (average of 58 experiments, where the uncertainty indicated corresponds to the standard deviation of the mean).

According to the literature,[29] the melting of cellobiose is accompanied by decomposition. We found an onset at $T_{on} = (236.4 \pm 0.7)$ °C

and a maximum intensity of the DSC melting peak at T_{max} = (241.9 ± 0.7) °C, in good agreement with the values published in the literature.[29–31] The calorimetric glass transition temperature in the lyophilized cellobiose was found to be T_g = 99 °C with a heat capacity jump ΔC_p = (0.38 ± 0.01) J K^{-1} g^{-1} = (132.2 ± 3.3) kJ mol^{-1}. This T_g value is higher than some values reported in the literature (T_g = 62 °C and T_g = 77 °C[31]), but in reasonable agreement with the one published by Miller and co-workers[28] (T_g = 108.1 °C).

3.1. Molecular mobility in amorphous cellobiose and gentiobiose

The amorphous samples were studied by TSDC in the temperature range between −165 °C and 125 °C (108–398 K). Both amorphous samples show a broad sub-T_g relaxation peak that extends from the lower accessible temperature (−165 °C) to room temperature, as presented in Figure 2. Let us note from the figure that this broad and well-defined sub-T_g relaxation peak, which is not present in the crystalline phases, displays a clear structure with different intensities in different temperature regions, revealing a hierarchy of the molecular motions.

The activation enthalpies of the partial polarization components of the molecular mobility shown in Figure 2 are displayed in Figure 3 for gentiobiose (full triangles) and cellobiose (full circles) as a function of the peak's location, T_m. The activation enthalpies were found to be distributed between 29 and 48 kJ mol^{-1} for both molecules, in agreement with the values of the Arrhenius activation energy of (32.8 ± 0.5) kJ mol^{-1} for cellobiose and (34.0 ± 1.0) kJ mol^{-1} for gentiobiose reported by Meißner[32] and obtained by dielectric relaxation spectroscopy.

Since the points are in the proximity of the line describing the zero entropy behavior, we conclude that we are in the presence of a secondary relaxation, that is, that these molecular mobility modes corresponding to the peaks in Figure 2 are low amplitude motions with a localized and non-cooperative nature.

Besides the secondary relaxation referred before, the TSDC spectrum of gentiobiose and cellobiose also showed another sub-T_g process in the temperature range between 20 and 90 °C (293–363 K, see Fig. 4). However, this relaxation peak showed a poor reproducibility, with intensity and shape changing significantly even if the experimental protocol was the same, so that we cannot ensure that it corresponds to a true dipolar relaxation. A relaxation with similar features was reported previously for trehalose[16] and D-salicin.[33] The analysis of the partial polarization peaks indicated

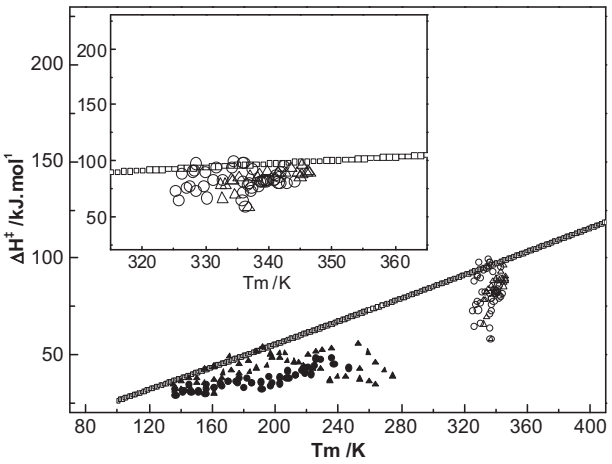

Figure 3. Activation enthalpy of the partial polarization peaks of the slow mobility of amorphous gentiobiose and cellobiose, as a function of the peak location, T_m. Full symbols (circles for cellobiose and triangles for gentiobiose) are relative to the slow mobility represented in Figure 2. Open symbols (circles and triangles, respectively, for cellobiose and gentiobiose) are relative to the mobility found at higher temperature, which is represented in Figure 4. The continuous line corresponds to the zero entropy prediction.

that the motional modes have activation enthalpies distributed between 70 and 120 kJ mol^{-1} and negligible activation entropies. In Figure 3 the empty triangles refer to amorphous gentiobiose and the empty circles refer to amorphous cellobiose. Pre-T_g signals have also been observed by DSC, which seem to correspond to thermally activated processes (the temperature location of the signals increases with increasing heating rate).[34,35] The attribution of these signals at the molecular level is however a controversial subject.

Another unexpected TSDC result found in amorphous cellobiose and gentiobiose is the absence of any relaxation peak attributable to the glass transition relaxation. In fact, no depolarization signal is observed in the temperature region where the glass transition peak should appear (90–100 °C). This behavior found for cellobiose and gentiobiose was also observed and reported before for trehalose[16] and D-salicin.[33] There are some indications in the literature that eventually corroborate (but do not explain) our intriguing observation. For example, the statements that 'in contrast to glucose, trehalose samples did not exhibit α-relaxation peaks'[36] and, in the same paper, that 'attempts to remove this component (conductiv-

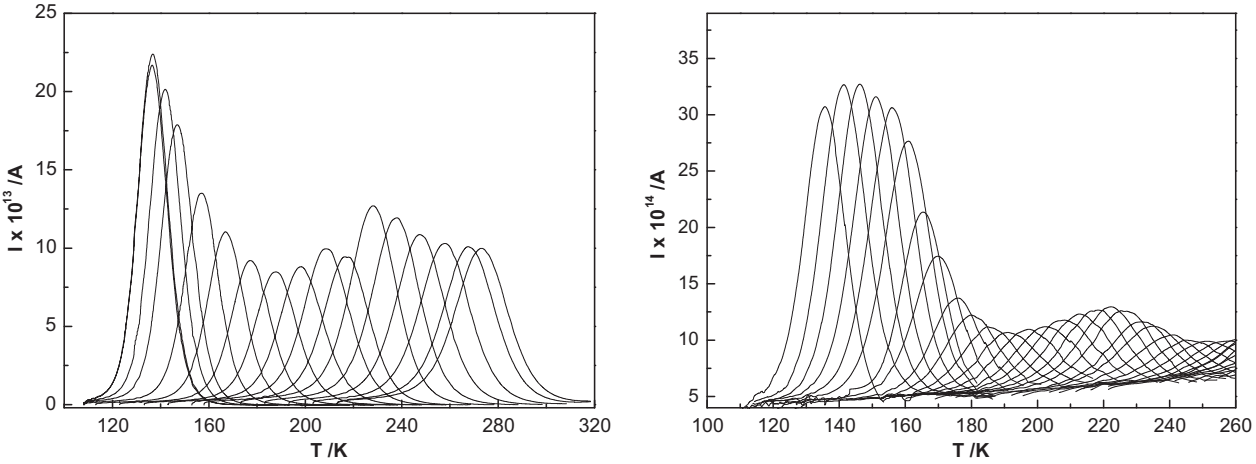

Figure 2. Partial polarization components of the slow mobility of amorphous gentiobiose (left) and cellobiose (right) obtained with polarization temperatures from 143 to 268 K in the case of gentiobiose and from 133 to 268 K in the case of cellobiose, with intervals of 5 K. Experimental conditions: strength of the polarization field E_p = 450 V mm^{-1}; polarization time t_p = 5 min; width of the polarization window ΔT = 2 K; heating rate r = 4 K min^{-1}.

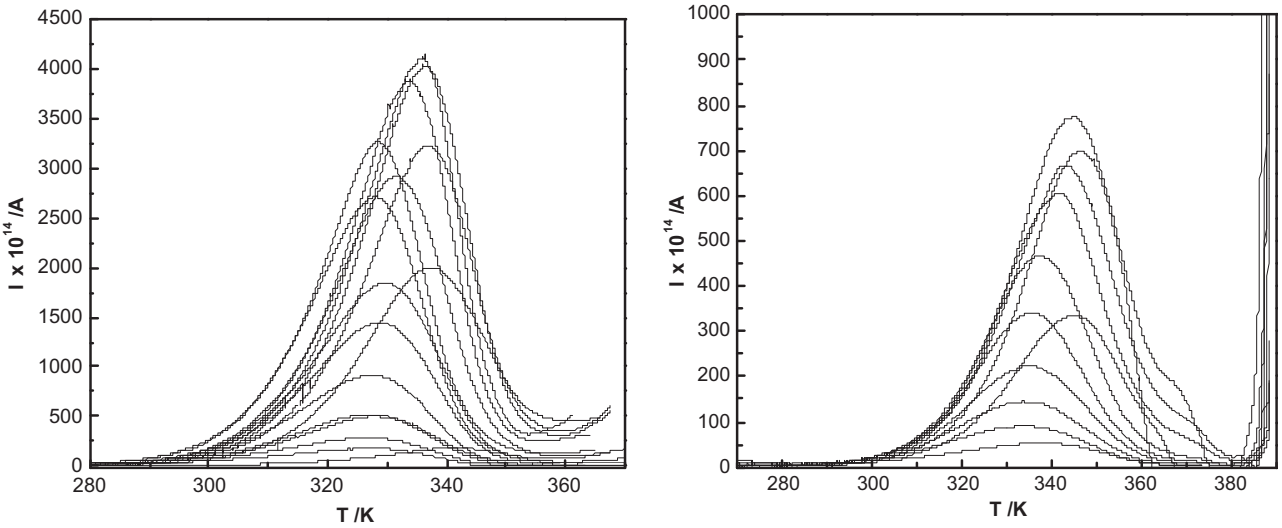

Figure 4. Partial polarization components of the slow mobility of amorphous gentiobiose (left) and cellobiose (right) obtained with polarization temperatures from 303 to 353 K in the case of gentiobiose and from 293 to 323 K in the case of cellobiose, with alternated intervals of 2 and 3 K. Experimental condition: strength of the polarization field E_p = 450 V mm^{-1}; polarization time t_p = 5 min; width of the polarization window ΔT = 2 K; heating rate r = 4 K min^{-1}.

ity) by purification of the sample or subtraction of the dc conductivity failed to reveal any underlying α-peaks'. Let us finally note that cellobiose, gentiobiose, and trehalose are disaccharides with two glucose constituent units, but with different position and type of glycosidic linkage between them, suggesting that their common behavior arises from structural factors. Moreover, it was also found that the primary or α-relaxation, which is directly connected to the glass transition, was not observed in cellulosic materials studied by dielectric relaxation spectroscopy,[37,38] and it was not detected by TSDC in ethyl cellulose[39] since it was hidden by a conductivity tail.

3.2. Molecular mobility in crystalline cellobiose and gentiobiose

A complex relaxation peak was found in both crystalline cellobiose and gentiobiose. The partial polarization peaks in Figure 5 correspond to the motional modes of gentiobiose (left) and cellobiose (right) in the crystalline phase. A conductivity tail is apparent at high temperatures. The analysis of the partial polarization peaks shown in Figure 5 indicates that all mobilities found in crystalline cellobiose and gentiobiose have similar kinetic parameters: activation enthalpies distributed between 70 and 125 kJ mol^{-1}, negligi-

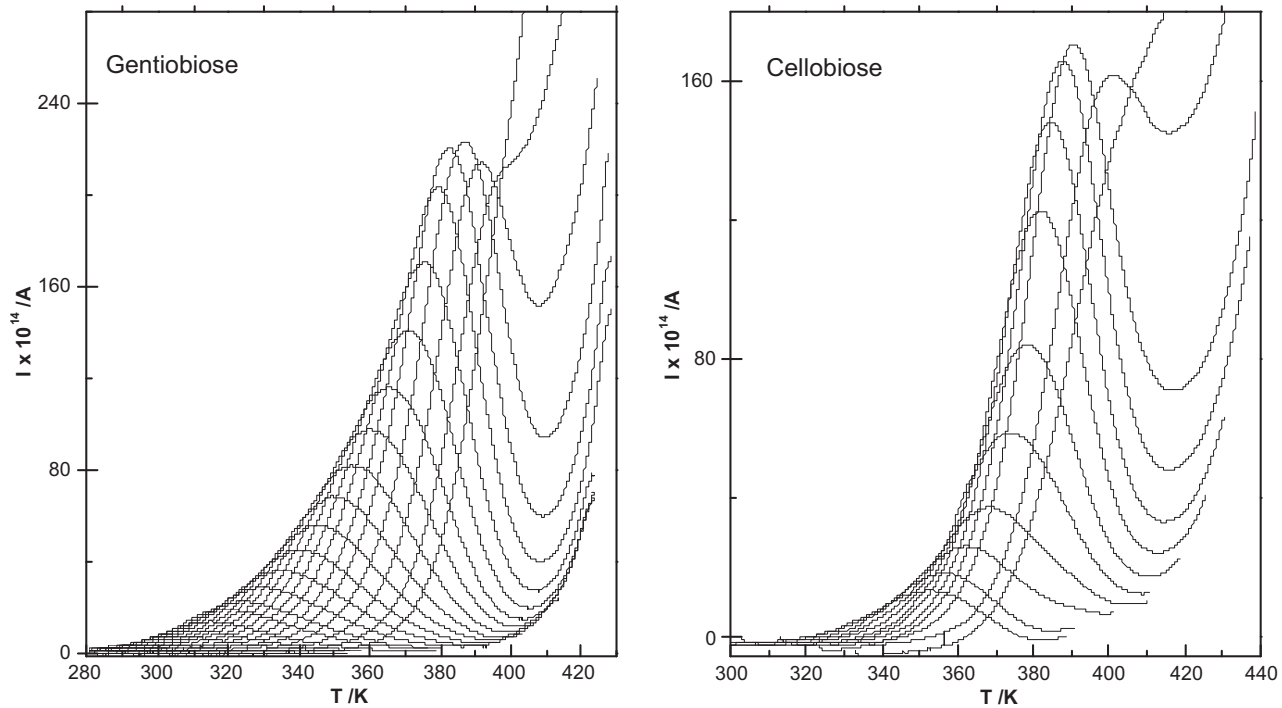

Figure 5. Partial polarization components of the slow mobility of crystalline gentiobiose (left) and cellobiose (right) obtained with polarization temperatures from 273 to 428 K in the case of gentiobiose and from 343 to 403 K in the case of cellobiose, with intervals of 5 K. Experimental conditions: strength of the polarization field E_p = 450 V mm^{-1}; polarization time t_p = 5 min; width of the polarization window ΔT = 2 K; heating rate r = 4 K min^{-1}.

ble activation entropies. These parameters are consistent with a local and non-cooperative mobility.[40,41]

3.3. Aging effect on the secondary relaxation of gentiobiose

It is now well established that, among the so-called secondary mobility, the Johari–Goldstein (JG) relaxation[42] has specific features, different from the trivial intramolecular character.

The JG relaxation corresponds to a sub-T_g small amplitude mobility, with a localized and non-cooperative nature, but it is believed that it depends on the intermolecular interactions and involves certain motions of the entire molecule as a whole.[43] Several criteria exist to identify a JG relaxation.[43] In recent works we proposed a methodology to distinguish the Johari–Goldstein relaxation from the other secondary relaxations, which is based on the study by thermally stimulated depolarization currents of the effect of physical aging on the secondary relaxations.[16,44,45]

In order to study the effect of aging on different motional components of the complex secondary relaxation of gentiobiose (Fig. 2) we choose two different partial polarization windows (with different temperature locations in the TSDC spectrum) as probes to monitor the evolution of the different mobilities with aging. Prior to each experiment the sample was annealed at T_a = 70 °C (343 K, 16° below the calorimetric glass transition, T_g) for different periods of aging time, t_a (usually 2, 5, 15, 30, 60, and 120 min). The two probes were the partial polarization windows with T_p = −130 °C (143 K) and −60 °C (213 K). Figure 6 shows the results of the effect of aging time on the probe experiments. From this figure we can conclude that the higher temperature probe is influenced by aging while the lower temperature mobility is not. On the other hand, the aging effect on peak 2 in Figure 6 leads to a decrease in intensity (and area, i.e., in dielectric strength) as the aging time increases.

Since the Johari–Goldstein relaxation is affected by the thermal history and aging times[43], we believe that the faster motional modes, that appear at lower temperatures (peak 1 in Fig. 6), and that are not affected by aging, have an intramolecular origin. These are local internal rotations that occur without significant interference of the neighboring molecules. The slower motional modes that appear at higher temperatures (peak 2 in Fig. 6) and are affected by aging have probably an intermolecular origin and correspond to the genuine β-relaxation or Johari–Goldstein relaxation.

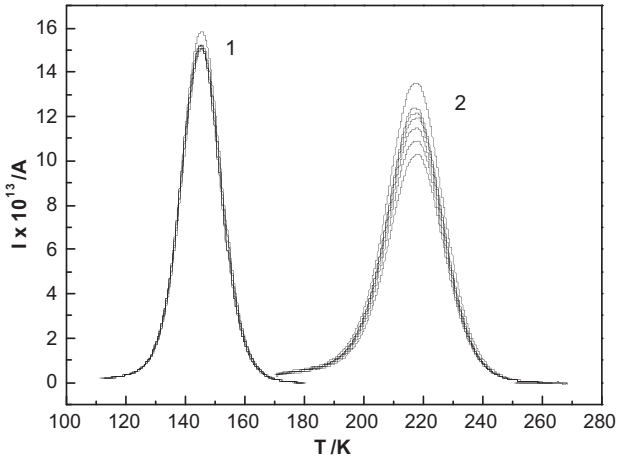

Figure 6. Effect of aging on different motional components of the secondary relaxation of gentiobiose (partial polarization probes at T_p = 143 and 213 K). Experimental condition: strength of the polarization field E_p = 450 V mm^{-1}; polarization time t_p = 5 min; width of the polarization window ΔT = 2 K; heating rate r = 4 K min^{-1}; the aging temperature were T_a = 343 K and the aging times were, in order of decrease intensity, t_a = 0, 2, 5, 15, 30, 60 and 120 min. Since the temperature never exceeded the 343 K in all experiments, the degree of aging of the sample accumulates, so that the effective aging time corresponds to the successive experiments is $(t_a)_{eff}$ = 0, 2, 7, 22, 52, 112 and 232 min.

From Figure 6 we also observe that the temperature location, T_m (temperature of maximum intensity), of the probing peak 2 of the Johari–Goldstein relaxation appears as essentially independent of the aging time. This behavior was also found in other glass formers such as trehalose[16], sorbitol[45], iditol[44], ethyl cellulose[39], and poly(-vinyl acetate).[46] Oppositely, aging affects the temperature location of the TSDC peaks of the main relaxation.[47–49] This observation indicates that the distribution of the relaxation times of the α-relaxation is modified by aging while that of the Johari–Goldstein relaxation is not.

3.4. Glass transition and fragility

As underlined in a previous section the technique of thermally stimulated depolarization currents is not able to detect any relaxation peak attributable to the glass transition relaxation in amorphous cellobiose and gentiobiose. However, the calorimetric signature of the main relaxation of these two glass formers can be easily and clearly obtained by differential scanning calorimetry (DSC). We thus decided to use DSC to characterize the glass transition in cellobiose and gentiobiose.

The dependence of T_g on heating or cooling rate of a DSC experiment allows the determination of the activation energy of structural relaxation at T_g, $E_a(T_g)$[50–52], according to

$$\frac{d\ln|q|}{d\,1/T_g} = -\frac{E_a}{R} \tag{1}$$

where E_a is the activation energy for the relaxation times controlling the structural enthalpy relaxation. On the other hand, the fragility index of a glass-forming system can be estimated from the activation energy at the glass transition temperature. The fragility parameter, m, of a glass-forming system, was proposed by Angell and is defined as the slope of the log $\tau(T)$ versus T_g/T line at the glass transition temperature, that is, at $T = T_g$[53,54]

$$m = \left[\frac{d\log_{10}\tau(T)}{d(T_g/T)}\right]_{T=T_g} \tag{2}$$

where τ is the structural relaxation time which slows down to ~100 s at T_g. Eq. (2) can be expressed in terms of the apparent activation energy, E_a, as

$$m = \frac{1}{2.303}\left[\frac{E_a(T_g)}{RT_g}\right] \tag{3}$$

We will thus analyze the influence of the heating rate on the onset temperature, T_{on}, of the DSC glass transition signal. In order to use Eq. (1) to estimate the activation energy of structural relaxation at T_g, $E_a(T_g)$, the experimental protocol was such that the supercooled liquid was cooled down through T_g to the glassy state (vitrification) at the same rate as the subsequent reheating for the measuring heating ramp.[50] The results of our experiments on the influence of the heating rate on the onset temperature, T_{on}, of the glass transition signal of cellobiose and gentiobiose are shown in Figure 7 as an 'Arrhenius plot' ($\ln|q|$ as a function of $1/T$). A relatively large scattering of the data points is observed; however, the large number of these data points reveals the general linear tendency in both cases.

From the linear regression we obtained an activation energy of E_a = 400 kJ mol^{-1} (standard deviation of ±55 kJ mol^{-1}) for cellobiose and E_a = 412 kJ mol^{-1} (standard deviation of ±47 kJ mol^{-1}) for gentiobiose. The calculated values of the fragility index were m = 56 and 60, respectively (the values T_g = 372 K for cellobiose and T_g = 359 K for gentiobiose, at 10 K min^{-1} on heating, were con-

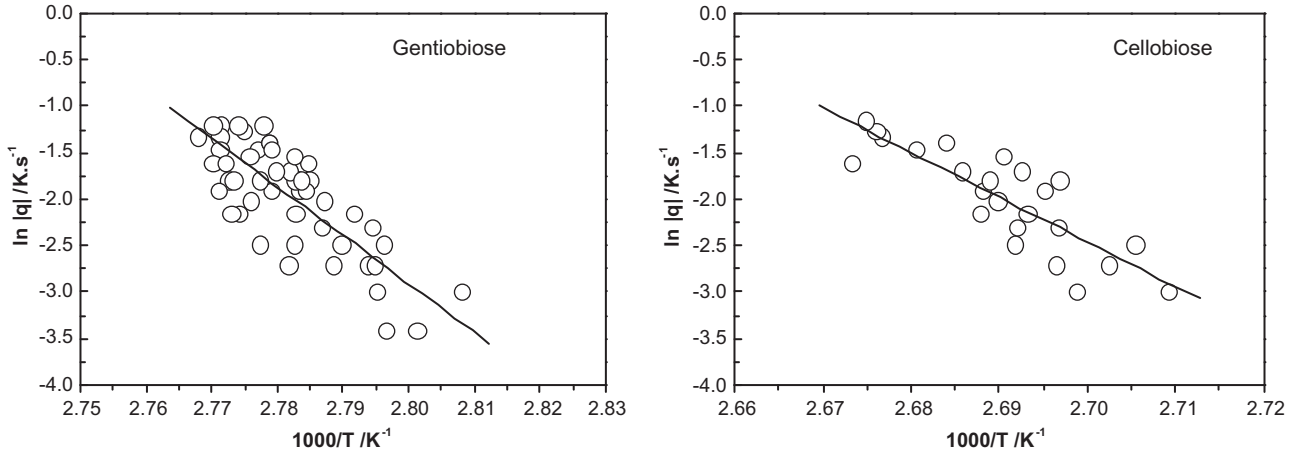

Figure 7. 'Arrhenius plot' (logarithm of the heating rate, q, as a function of $1/T_{on}$) for the glass transition of gentiobiose (left) and cellobiose (right) studied by DSC.

sidered in the calculation of m), indicating that these disaccharides are moderately fragile liquids.

4. Conclusions

The mobility in the amorphous solid cellobiose and gentiobiose showed a broad and complex secondary relaxation revealing a clear structuration with two kinds of molecular motions, and with activation energies distributed between 29 and 48 kJ mol^{-1}. It was found that the lower temperature components of this complex secondary mobility are aging independent and correspond to the γ or fast β-relaxation, while the higher temperature components are affected by aging and correspond to the slow β or Johari–Goldstein relaxation. An unexpected and intriguing feature of the TSDC thermogramme of cellobiose and gentiobiose is that no depolarization signal is present in the glass transformation region. Trehalose displays the same behavior. Research focused on this problem is needed to understand this uncommon behavior.

The steepness index or fragility, m, of cellobiose and gentiobiose was determined by DSC based on the scanning rate dependency of T_g, indicating that these disaccharides are moderately fragile liquids.

Reference

1. Fox, K. C.. *Science* **1995**, *267*, 1922–1923.
2. Crowe, L. M. *Comp. Biochem. Physiol. A Mol. Integr. Physiol.* **2002**, *131*, 505–513.
3. Lichtenthaler, F. W.; Peters, S. *Comptes Rendus Chim.* **2004**, *7*, 65–90.
4. Roberts, C. J.; Debenedetti, P. G. *AIChE J.* **2002**, *48*, 1140–1144.
5. Yu, L. *Adv. Drug Deliv. Rev.* **2001**, *48*, 27–42.
6. Andronis, V.; Zografi, G. *Pharm. Res.* **1997**, *14*, 410–414.
7. Bhattacharya, S.; Suryanarayanan, R. *J. Pharm. Sci.* **2009**, *98*, 2935–2953.
8. Wungtanagorn, R.; Schmidt, S. J. *Thermochim. Acta* **2001**, *369*, 95–116.
9. Hancock, B. C.; Shamblin, S. L.; Zografi, G. *Pharm. Res.* **1995**, *12*, 799–806.
10. Green, J. L.; Angell, C. A. *J. Phys. Chem.* **1989**, *93*, 2880–2882.
11. Nakamura, S.; Oku, T.; Ichinose, M. *Nutrition* **2004**, *20*, 979–983.
12. Nakamura, S. *Nutrition* **2005**, *21*, 1158–1159.
13. Benton, R. *LC-GC North America* **2005**, 54.
14. Yang, B.; Guo, Z.; Liu, R. *Tsinghua Sci. Technol.* **2005**, *10*, 567–572.
15. Diogo, H. P.; Moura Ramos, J. J. *Carbohydr. Res.* **2008**, *343*, 2797–2803.
16. Moura Ramos, J. J.; Pinto, S. S.; Diogo, H. P. *ChemPhysChem* **2007**, *8*, 2391–2396.
17. Saito, T., Hayamizu, K., Yanagisawa, M., Yamamoto, O., Wasada, N., Someno, K., Kinugasa, S., Tanabe, K., Tamura, T., and Hiraishi, J., Spectral data base for organic compounds, http://riodb.ibase.aist.go.jp/riohomee.html, 2010.
18. Chu, S. S. C.; Jeffrey, G. A. *Acta Cryst., Sect. D* **1968**, *24*, 830–838.
19. Teyssedre, G.; Lacabanne, C. *J. Phys. D: Appl. Phys.* **1995**, *28*, 1478–1487.
20. Correia, N. T.; Alvarez, C.; Moura Ramos, J. J.; Descamps, M. *J. Phys. Chem. B* **2001**, *105*, 5663–5669.
21. van Turnhout, J. *Thermally Stimulated Discharge of Polymer Electrets*; Elsevier Sci. Pub.: Amsterdam, 1975.
22. Chen, R.; Kirsch, Y. *Analysis of Thermally Stimulated Processes*; Pergamon Press: Oxford, 1981.
23. Teyssedre, G.; Mezghani, S.; Bernes, A.; Lacabanne, C. In *Thermally Stimulated Currents of Polymers*; Runt, J. P., Fitzgerald, J. J., Eds.; American Chemical Society: Washington, 1997.
24. Sauer, B.B. Thermally Stimulated Currents: recent developments in characterisation and analysis of polymers. In Handbook of Thermal Analysis and Calorimetry; Gallager, P. K., Ed. In *Applications to polymers and plastics*; Cheng, S. Z. D. Ed.; Elsevier: Amsterdam, 2002; pp 653–711.
25. Correia, N. T.; Moura Ramos, J. J.; Descamps, M.; Collins, G. *Pharm. Res.* **2001**, *18*, 1767–1774.
26. Moura Ramos, J. J.; Correia, N. T.; Diogo, H. P. *Chem. Educ.* **2009**, *14*, 175–179.
27. Moura Ramos, J. J.; Taveira-Marques, R.; Diogo, H. P. *J. Pharm. Sci.* **2004**, *93*, 1503–1507.
28. Miller, D. P.; de Pablo, J. J. *J. Phys. Chem. B* **2000**, *104*, 8876–8883.
29. Hatakeyama, T.; Yoshida, H.; Nagasaki, C.; Hatakeyama, H. *Polymer* **1976**, *17*, 559–562.
30. Wolfrom, M. L.; Dacons, J. C. *J. Am. Chem. Soc.* **1952**, *74*, 5331–5333.
31. Slade, L.; Levine, H. *Pure Appl. Chem.* **1988**, *60*, 1841–1864.
32. Meißner, D.; Einfeldt, J.; Kwasniewski, A. *J. Non-Cryst. Solids* **2000**, *275*, 199–209.
33. Diogo, H. P.; Pinto, S. S.; Moura Ramos, J. J. *Int. J. Pharm.* **2008**, *358*, 192–197.
34. Luthra, S. A.; Hodge, I. M.; Pikal, M. J. *J. Pharm. Sci.* **2008**.
35. Vyazovkin, S.; Dranca, I. *J. Phys. Chem. B* **2007**, *111*, 7283–7287.
36. Cummins, H. Z.; Zhang, H. P.; Oh, J. Y.; Seo, J. A.; Kim, H. K.; Hwang, Y. H.; Yang, Y. S.; Yu, Y. S.; Inn, Y. *J. Non-Cryst. Solids* **2006**, *352*, 4464–4474.
37. Einfeldt, J.; Meißner, D.; Kwasniewski, A. *Cellulose* **2004**, *11*, 137–150.
38. Einfeldt, J.; Meißner, D.; Kwasniewski, A. *Progr. Polym. Sci.* **2001**, *26*, 1419–1472.
39. Diogo, H. P.; Moura Ramos, J. J. *J. Polym. Sci. B: Polym. Phys.* **2009**, *74*, 820–829.
40. Starkweather, H. W. *Macromolecules* **1988**, *21*, 1798–1802.
41. Starkweather, H. W. *Polymer* **1991**, *32*, 2443–2448.
42. Johari, G. P.; Goldstein, M. *J. Chem. Phys.* **1970**, *53*, 2372–2388.
43. Ngai, K. L.; Paluch, M. *J. Chem. Phys.* **2004**, *120*, 857–873.
44. Moura Ramos, J. J.; Diogo, H. P.; Pinto, S. S. *Thermochim. Acta* **2008**, *467*, 107–112.
45. Moura Ramos, J. J.; Diogo, H. P.; Pinto, S. S. *J. Chem. Phys.* **2007**, *126*, 144506-1–144506-6.
46. Pinto, S. S.; Moura Ramos, J. J.; Diogo, H. P. *Eur. Polym. J.* **2009**, *45*, 2644–2652.
47. Correia, N. T.; Alvarez, C.; Moura Ramos, J. J.; Descamps, M. *J. Chem. Phys.* **2000**, *113*, 3204–3211.
48. Descamps, M.; Moura Ramos, J. J.; Correia, N. T. *Mol. Phys.* **2002**, *100*, 2669–2677.
49. Diogo, H. P.; Moura Ramos, J. J. *J. Mol. Liq.* **2006**, *129*, 138–146.
50. Moynihan, C. T.; Easteal, A. J.; Wilder, J.; Tucker, J. *J. Phys. Chem.* **1974**, *78*, 2673–2677.
51. Crowley, K. J.; Zografi, G. *Thermochim. Acta* **2001**, *380*, 79–93.
52. Simatos, D.; Blond, G.; Roudaut, G.; Champion, D.; Perez, J.; Faivre, A. L. *J. Therm. Anal.* **1996**, *47*, 1419–1436.
53. Böhmer, R.; Angell, C. A. Local and Global Relaxations in Glass-Forming Materials. In *Disorder Effects on Relaxational Processes*; Richert, R., Blumen, A., Eds.; Springer: Berlin, 1994; pp 11–54.
54. Böhmer, R.; Ngai, K. L.; Angell, C. A.; Plazek, D. J. *J. Chem. Phys.* **1993**, *99*, 4201–4209.